Wnt5a-treated midbrain neural stem cells improve dopamine cell replacement therapy in parkinsonian mice

Clare L. Parish,[1] Gonçalo Castelo-Branco,[1] Nina Rawal,[1] Jan Tonnesen,[2,3] Andreas Toft Sorensen,[2,3] Carmen Salto,[1] Merab Kokaia,[2,3] Olle Lindvall,[2] and Ernest Arenas[1]

[1]Laboratory of Molecular Neurobiology, Department of Medical Biochemistry and Biophysics, Karolinska Institute, Stockholm, Sweden.
[2]Laboratory of Neurogenesis and Cell Therapy and [3]Experimental Epilepsy Group, Section of Restorative Neurology, Wallenberg Neuroscience Center, Lund University, Lund, Sweden.

Dopamine (DA) cell replacement therapy in Parkinson disease (PD) can be achieved using human fetal mesencephalic tissue; however, limited tissue availability has hindered further developments. Embryonic stem cells provide a promising alternative, but poor survival and risk of teratoma formation have prevented their clinical application. We present here a method for generating large numbers of DA neurons based on expanding and differentiating ventral midbrain (VM) neural stem cells/progenitors in the presence of key signals necessary for VM DA neuron development. Mouse VM neurospheres (VMNs) expanded with FGF2, differentiated with sonic hedgehog and FGF8, and transfected with Wnt5a (VMN-Wnt5a) generated 10-fold more DA neurons than did conventional FGF2-treated VMNs. VMN-Wnt5a cells exhibited the transcriptional and biochemical profiles and intrinsic electrophysiological properties of midbrain DA cells. Transplantation of these cells into parkinsonian mice resulted in significant cellular and functional recovery. Importantly, no tumors were detected and only a few transplanted grafts contained sporadic nestin-expressing progenitors. Our findings show that Wnt5a improves the differentiation and functional integration of stem cell–derived DA neurons in vivo and define Wnt5a-treated neural stem cells as an efficient and safe source of DA neurons for cell replacement therapy in PD.

Introduction

Parkinson disease (PD) is a common chronic neurodegenerative disorder characterized by tremor, rigidity, and hypokinesia. The main pathology is a progressive degeneration of substantia nigra neurons leading to severe loss of striatal dopamine (DA) innervation. Clinical trials with transplantation of human fetal mesencephalic tissue in PD patients have demonstrated that grafted DA neurons can reinnervate the denervated striatum (1), release DA (2), and become functionally integrated into host neural circuitries (3). However, the functional outcome after transplantation has been variable, depending in part on technical issues such as tissue quantity, quality, and preparation as well as immunosuppression (4–7). Although some patients showed limited clinical benefit and 15% of patients developed dyskinesias, others have experienced a remarkable improvement that allowed withdrawal of L-DOPA (8, 9).

A major technical limitation that has prevented rigorous testing and widespread application of neural transplantation is the need for tissue from approximately 6 fetuses to treat 1 patient (8). ES cells have emerged as an attractive cell source for cell replacement therapy in PD because of their capacity to generate large numbers of DA neurons and induce functional recovery in parkinsonian mice (10–12). However, the excessive proliferation, the risk for teratoma formation, and the poor survival of human ES cell–derived DA cells after transplantation in animal models have so far prevented their use in clinical trials (13–15). Taking advantage of recent advances in the understanding of DA neuron development, we aimed at devising a method to obtain DA-rich cell cultures that functionally integrate in vivo without risk of teratomas. Neurospheres provide a culture system to expand multipotent, self-renewing neural stem cells from the developing and adult brain. These spheres can be induced to proliferate in vitro by epigenetic means, i.e., through addition of mitogens such as FGF2 and epidermal growth factor as seen in forebrain (16, 17) or ventral midbrain (VM) cultures (18, 19). While such techniques in the VM can result in a 10-fold increase in the total number of cells, a 3-fold increase was seen in DA cell numbers in vitro and an estimated 0.3% of the transplanted cells adopted a DA phenotype (19). In another study, grafting of spheres generated from *nestin-GFP*–sorted mesencephalic progenitors induced a moderate functional recovery in PD animals (20). Combined, these studies suggested that neural stem/progenitor cultures need to be exposed to additional cues to improve DA differentiation and survival.

Early in development, floor plate cells in the ventricular zone of the VM secrete the ventralizing signal sonic hedgehog (Shh), while neuroepithelial cells of the isthmus secrete FGF8. Precise gradients of these 2 morphogens provide positional information and regulate the development of DA neurons in the VM, and alone are capable of inducing ectopic DA neurons (11, 21, 22). Additional, yet-unknown soluble signals are expected to enhance the phenotypic features and survival of DA neurons. We recently identified Wnt5a as a previously elusive VM glia-derived soluble factor capable of inducing DA differentiation in primary VM progenitor cell preparations in vitro (23–25). Moreover, we found that specific Wnt

Nonstandard abbreviations used: DA, dopamine, dopaminergic; GFAP, glial fibrillary acidic protein; GIRK2, G protein–coupled inward rectifying K^+ channel 2; 6-OHDA, 6-hydroxydopamine; PD, Parkinson disease; Pitx3, paired-like homeodomain transcription factor 3; Shh, Sonic hedgehog; SNpc, substantia nigra pars compacta; TH, tyrosine hydroxylase; VM, ventral midbrain; VMN, VM neurosphere.

Conflict of interest: The authors have declared that no conflict of interest exists.

Citation for this article: *J. Clin. Invest.* **118**:149–160 (2008). doi:10.1172/JCI32273.

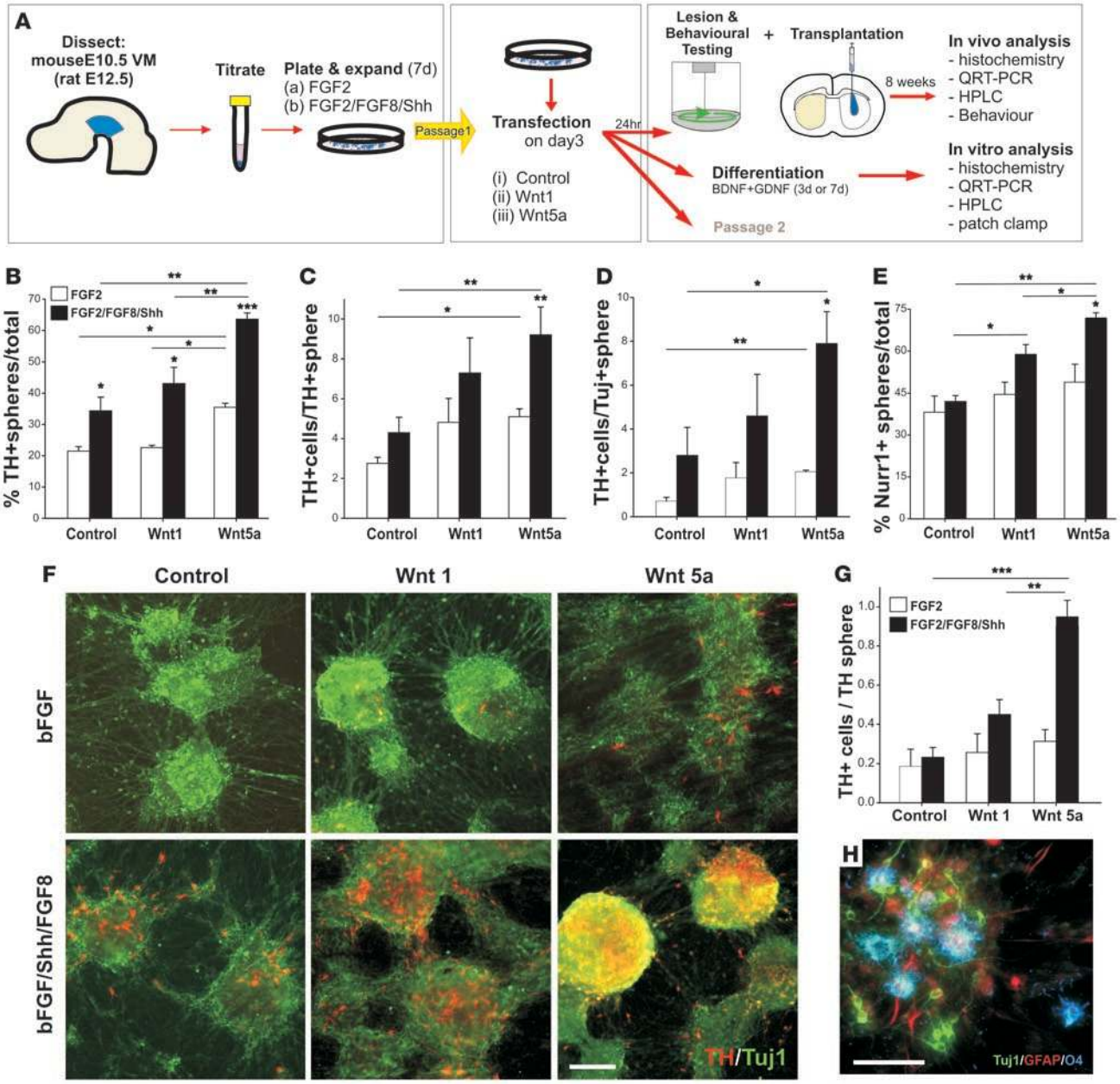

Figure 1

Expansion and DA differentiation of VMNs. (**A**) Experimental design. Isolated VM cells were expanded and patterned in vitro prior to transfection to overexpress Wnts. Cell phenotype was examined following in vitro differentiation or transplantation into parkinsonian mice. (**B**) Morphogens Shh and FGF8 significantly increased the proportion of TH$^+$ spheres out of total spheres compared with FGF2 treatment alone. The number of TH$^+$ neurons per VMN increased in the presence of morphogens in both passage 1 (**C**) and passage 2 cultures (**G**). Wnt overexpression had little effect on TH expression in FGF2-treated VMNs, while Wnt1, and more predominantly Wnt5a, enhanced both the percentage TH$^+$ per total spheres and the number of TH neurons per sphere in FGF2/Shh/FGF8 VMNs (**C** and **D**). (**E**) Percent Nurr1$^+$ spheres significantly increased compared with FGF2-treated spheres in response to Shh and FGF8 as well as Wnt proteins. Note that Wnt1 increased the percentage of Nurr1$^+$ spheres (**E**) but not TH$^+$ spheres per total (**B**), suggesting lack of specificity of proliferation in all precursor cells, while Wnt5a increased both Nurr and TH/Tuj1/βIII-tubulin, indicating selective increased differentiation of Wnt5a-FGF2/Shh/FGF8–treated VMNs. (**F**) Photomicrographs of VMNs treated with FGF2 or FGF2/Shh/FGF8 and Wnt1 or Wnt5a. (**G**) Similar trends in the regulation of TH$^+$ cell numbers were noted in passage 2 cultures compared to passage 1; however, the percentage of TH$^+$ cells per sphere was reduced with subsequent passaging. (**H**) Clonal analysis of VMN cells identified multipotent sphere-initiating neural stem cells that gave rise to neurons (Tuj1/βIII-tubulin), astrocytes (GFAP), and oligodendrocytes (O4) after differentiation. $^*P < 0.05$; $^{**}P < 0.01$; $^{***}P < 0.001$. Scale bars: 200 μm (**F**); 100 μm (**H**).

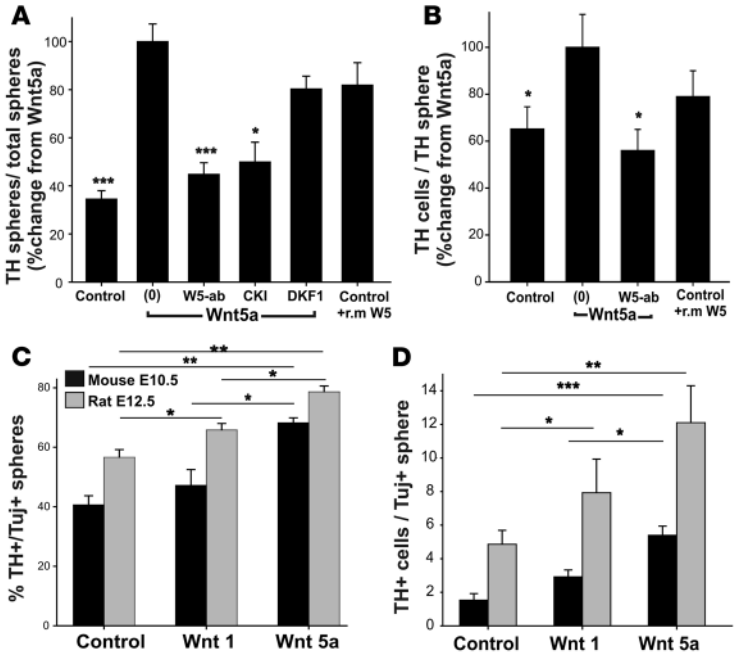

Figure 2
Wnt5a mediates effects on DA differentiation via noncanonical signaling across rodent species. (**A** and **B**) Effects of Wnt5a overexpression were abolished by using a Wnt5a-blocking antibody (W5-ab) or the D4476 CKI inhibitor (CKI), but not the canonical Wnt blocker dickkopf-1 (DKF1). Mouse recombinant Wnt5a protein (r.m.W5) induced effects comparable to those of Wnt5a overexpression in control-transfected spheres. (**C** and **D**) Comparable trends for number of TH$^+$ cells per sphere (**C**) and percentage of TH$^+$ spheres per Tuj1/βIII-tubulin$^+$ spheres (**D**) were observed in E12.5 rat compared with E10.5 mouse cultures. However, significantly more TH$^+$ cells were present in rat cultures than in mouse cultures. Data are mean ± SD (n = 4). *P < 0.05; **P < 0.01; ***P < 0.001, 1-way ANOVA with Tukey post-hoc test.

proteins promote the development of midbrain DA cells in vitro by distinct mechanisms (24, 26, 27). Wnt1 primarily contributes to the specification of DA progenitors and neurogenesis within the midbrain, while Wnt5a predominantly increases differentiation of Nurr1$^+$ precursors into DA neurons (24, 26). Using these signals we have developed a method to effectively expand and differentiate VM neurospheres (VMNs) into DA neurons as a source of cells for cell replacement therapy in PD.

Results

VM tissue was isolated from mice at E10.5, just prior to/at the onset of birth of DA cells, and the total number of cells in the cultures was expanded 2- to 3-fold for 1 passage as VMNs in the presence of FGF2 alone or together with FGF8 and Shh. These cells were subsequently transfected with control, Wnt1, or Wnt5a plasmids prior to in vitro and in vivo analysis (Figure 1A). Compared with FGF2 alone, treatment with FGF2/FGF8/Shh induced a significant increase in spheres immuoreactive to tyrosine hydroxylase (TH; the rate-limiting enzyme in DA synthesis) relative to total spheres (Figure 1, B and F). However, it did not significantly increase the number of TH$^+$ cells per sphere positive for TH (Figure 1C) or for Tuj1/βIII-tubulin, a cytoskeletal neuronal protein (Figure 1D). More noteworthy were the effects of Wnts on the number of TH cells. In the presence of FGF2/Shh/FGF8, but not FGF2 alone, Wnt1 significantly increased the percentage of spheres positive for Nurr1, a marker for postmitotic DA precursors and neurons (Figure 1E). Wnt1 had no effect on the percentage of TH$^+$ spheres per total spheres or TH$^+$ cells per Tuj1/βIII-tubulin$^+$ spheres compared with control (Figure 1, B and D), suggesting that Wnt1 increases the number of DA precursors but does not specifically enhance DA neurons. Strikingly, Wnt5a induced a greater increase in the percentage of TH$^+$ and Nurr1$^+$ spheres (Figure 1, B and E) and greatly enhanced the number of TH$^+$ cells per TH$^+$ or Tuj1/βIII-tubulin$^+$ sphere (Figure 1, C, D, and F), indicating a more specific effect of Wnt5a on DA differentiation than observed with Wnt1. Therefore, in the presence of Shh and FGF8, Wnt5a increased both the frequency of TH$^+$ spheres (3-fold) and the number of TH$^+$ cells within the TH$^+$ spheres (3.3-fold) to induce approximately a 10-fold increase in the yield of TH cells compared with FGF2 treatment.

We subsequently examined the properties of the neurospheres in terms of formation of secondary spheres, capacity to give rise to dopaminergic neurons, and multilineage differentiation potential in clonal conditions. With regard to dopaminergic differentiation, we noted similar trends in the regulation of TH$^+$ cell numbers by Wnts, which depended on the presence of Shh and FGF8 treatment, in both passage 1 and 2 cultures (Figure 1, C and G). However, the number of TH$^+$ cells per sphere was reduced with subsequent passaging, indicating that the expansion/differentiation capacity of VM dopaminergic progenitors is limited under the present culture conditions. Clonal analysis revealed that 9.3% of cells in a neurosphere gave rise to secondary neurospheres. Moreover, we found that 5-day differentiation of neurospheres derived from a single cell gave rise to cells expressing neuronal (βIII-tubulin), astrocytic (glial fibrillary acidic protein; GFAP), and oligodendrocytic (O4) markers (Figure 1H). These findings illustrate that multipotent sphere-initiating neural stem cells are present in the culture.

In order to confirm the effects of Wnt5a, we treated FGF2/Shh/FGF8-expanded spheres with Wnt5a recombinant protein. Treatment with pure Wnt5a protein induced the same effects as Wnt5a overexpression (Figure 2, A and B). We subsequently tested the specificity of the effect of Wnt5a in more detail by performing a blocking experiment with a Wnt5a antibody. We found that the Wnt5a antibody completely blocked the effects of Wnt5a overexpression, suggesting that Wnt5a is required for the effects on TH$^+$ cells (Figure 2, A and B). Next, we wished to determine the mechanism by which Wnt5a leads to an increase in TH$^+$ cells and whether Wnt5a activates canonical or noncanonical Wnt signaling. We found that Dickkopf-1 (an inhibitor of canonical Wnt signaling; ref. 28) had no significant effects on the number of TH$^+$ spheres in culture (Figure 2A), suggesting that the canonical Wnt signaling pathway is not involved. Instead, D4476, a CKI inhibitor that blocks both canoni-

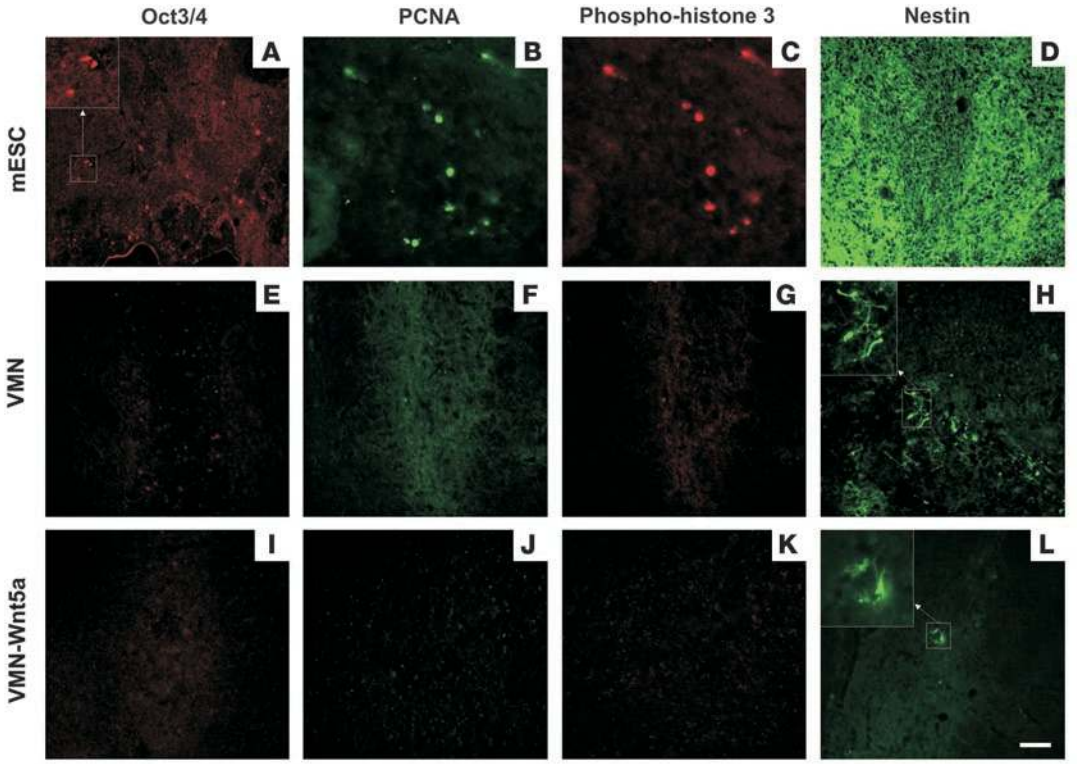

Figure 3
VMN-Wnt5a grafts show no signs of tumor formation, proliferation, or cell expansion. Animals grafted with predifferentiated mouse ES cells (mESC) showed immunoreactivity for various markers of proliferating cells types including Oct3/4 (**A**), PCNA (**B**), and phospho–histone-3 (**C**), which were not seen in VMN and VMN-Wnt5a grafts (**E**–**G** and **I**–**K**, respectively). (**D**) Additionally, mouse ES cell grafts showed dense regions of nestin$^+$ cells. Extremely few nestin$^+$ cells were seen in very small clusters in select VMN grafts (**H**), and isolated nestin$^+$ cells were observed in fewer VMN-Wnt5a grafts (**L**). Scale bar: 100 μm.

cal and noncanonical Wnt signaling (29), blocked the increase in percentage of TH$^+$ spheres induced by Wnt5a overexpression (Figure 2A). Furthermore, no change in active β-catenin was observed in Wnt5a-overexpressing cultures compared with control (Supplemental Figure 1; available online with this article; doi:10.1172/JCI32273DS1). Thus, our results suggest that the effect of Wnt5a on developing dopaminergic neurons is mediated by noncanonical Wnt signaling. This finding is also supported by previous results showing activation of noncanonical Wnt signaling by Wnt5a in a dopaminergic cell line (30). We also examined the robustness of the effects of Wnt5a across species by comparing E10.5 mouse and E12.5 rat VMNs. Similar trends between passages and across species were detected in the proportion of TH$^+$ spheres (Figure 2C). However, rat cultures resulted in a further 2-fold increase in number of TH$^+$ cells per Tuj1/βIII-tubulin$^+$ sphere (Figure 2D) compared with the same condition in mice. Therefore, rat cultures were used for transplantation and functional assessment in vivo.

The ability of rat VMN and VMN-Wnt5a cells (cultured in the presence of FGF2/Shh/FGF8) to survive, integrate, and induce functional recovery (without tumor formation) after transplantation was examined in parkinsonian nude mice lesioned by 6-hydroxydopamine (6-OHDA). At the histological level, we first confirmed that all animals included in the study had near-complete lesions of the substantia nigra pars compacta (SNpc; cell loss >90%; data not shown), and had viable grafts at 8 weeks after transplantation. More importantly, no grafted animals showed any signs of tumor formation. Assessment of various markers for undifferentiated and proliferating cells types revealed no pluripotent stem cells (Oct3/4$^+$) or proliferating cells (phospho-histone-3$^+$ or proliferating cell nuclear antigen–positive [PCNA$^+$] cells) within VMN or VMN-Wnt5a grafts, as seen occasionally in grafts originating from mouse ES cells predifferentiated with Shh and FGF8 on PA6 (Figure 3). Moreover, VMN and VMN-Wnt5a grafts showed extremely few nestin$^+$ cells only occurring within some grafts, their numbers being dramatically lower compared with ES cell grafts (Figure 3, D, H, and L). Thus, our results support the notion that VMN grafts are safer for cell replacement therapy than ES cells since undifferentiated, mitotically active, neuroepithelial cells are not expanded and do not give rise to tumors.

At the behavioral level, animals receiving VMN grafts for 8 weeks exhibited a significant improvement in motor behavior as revealed by amphetamine and apomorphine rotational tests (56% and 55% reduction of asymmetry, respectively; Figure 4, A and B). Already at 4 weeks, and subsequently at 6 and 8 weeks, VMN-Wnt5a–transplanted animals showed more pronounced improvement in behavior compared with VMN-transplanted mice. By 8 weeks, VMN-Wnt5a animals exhibited full functional recovery, as assessed by both amphetamine (101%) and apomorphine (83%) testing (Figure 4, A and B). In contrast, sham-grafted animals showed no significant behavioral improvements. Next, we assessed whether the behavioral improvement correlated with the number of TH$^+$ neurons within the graft site. VMN-transplanted animals

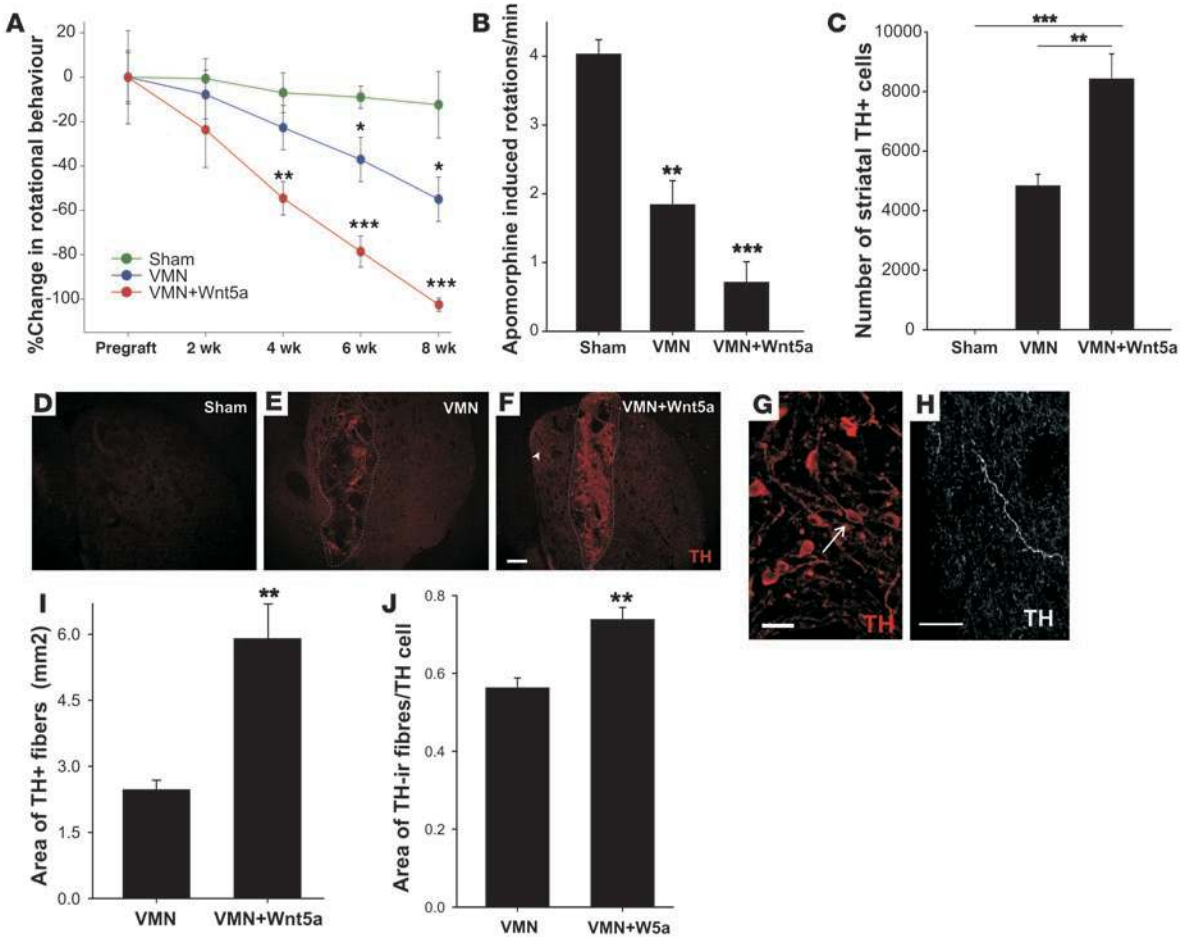

Figure 4

Transplantation of Wnt5a-overexpressing VMNs induces behavioral and cellular recovery in parkinsonian mice. (**A**) Time course of amphetamine-induced rotational behavior in sham-, VMN-, and VMN-Wnt5a–grafted animals. VMN transplants resulted in significant behavioral improvement at 8 weeks, while VMN-Wnt5a transplants resulted in full restoration of behavior. (**B**) Confirmation of behavioral improvements following apomorphine-induced rotational testing at 8 weeks. (**C**) Number of TH^+ cells within the striatum of grafted animals. (**D**–**F**) Photomicrographs in the striatum of grafts from sham-operated (**D**), VMN-grafted (**E**), and VMN-Wnt5a–grafted (**F**) mice. (**G**) High-power image of DA neurons residing within a VMN-Wnt5a graft showing classical bipolar morphology (arrow). (**H**) High-power image of a hypertrophied TH^+ fiber located outside the graft site (arrowhead in **F**). (**I**) Area of TH-immunoreactive fibers within the striatum following grafting. (**J**) Area of fibers per TH cell. Note that regardless of the increase in cell numbers, the density of fibers per cell in VMN-Wnt5a grafts was significantly greater, suggesting neuritogenesis and greater integration into the host tissue. Data are mean ± SD ($n = 6$ per group). $^*P < 0.05$; $^{**}P < 0.01$; $^{***}P < 0.001$, ANOVA with Tukey post-hoc test. Scale bars: 200 μm (**D**–**F**); 50 μm (**G**); 100 μm (**H**).

had 4,831 ± 391 TH^+ cells, significantly fewer than the 8,422 ± 816 TH^+ cells seen in VMN-Wnt5a grafts (Figure 4, C–F). These counts reflected 6.4% and 9.5% of total cells (TH/Hoechst) surviving by 8 weeks within VMN and VMN-Wnt5a graft, respectively. Similarly, average graft volume occupied by TH^+ immunoreactive fibers was significantly higher in VMN-Wnt5a compared with VMN grafts (Figure 4I). Moreover, upon closer examination, we noticed that the area of TH^+ fibers per TH^+ cell was significantly greater in VMN-Wnt5a grafts, indicating that the sprouting per TH cell was enhanced by Wnt5a (Figure 4J). Numerous hypertrophied fibers were seen at long distances away from the graft site, raising the possibility that these Wnt5a-treated cells also integrated better into the host tissue (Figure 4H). These histological and behavioral findings led us to hypothesize that Wnt5a treatment of VMNs may allow for a reduction in the number of cells and donors necessary to treat 1 parkinsonian mouse compared with control VMNs. We explored the possibility that grafting twice as many control cells would induce the same results seen from our VMN-Wnt5a cells. We found that 800,000 VMN cells caused behavioral and histological recovery similar to that observed with 400,000 VMN-Wnt5a cells (Figure 5). These results confirm our hypothesis that VMN-Wnt5a cells are twice as efficient as control VMN cells for DA cell replacement and show that half the VMN-Wnt5a cells are sufficient to obtain a similar number of TH^+ cells in vivo and degree of behavioral recovery.

We next examined the mechanism by which Wnt5a increased the number of DA neurons in vivo in mice grafted with 400,000 cells. We observed that a significant proportion of the $Nurr1^+$ cells in VMN grafts (39%) did not mature into TH^+ neurons (Figure 6, A–C). In contrast, the majority of $Nurr1^+$ cells (88%) in VMN-Wnt5a grafts differentiated into TH^+ neurons (Figure 6, B and D). A significant increase in total numbers of $Nurr1^+$ cells in VMN-Wnt5a

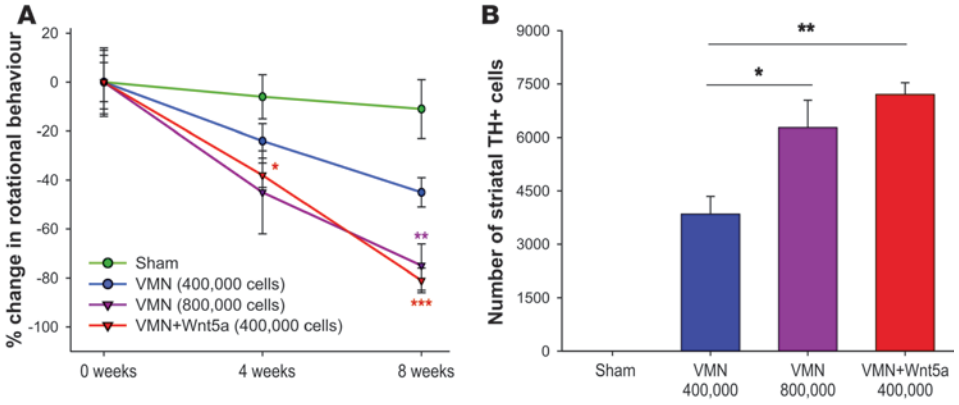

Figure 5
Wnt5a reduces the number of cells required for functional engraftment in PD mice. Transplantation of twice the number of VMN cells was required to induce similar behavioral and histological recovery as obtained with VMN-Wnt5a grafts (800,000 and 400,000 cells, respectively). Effects are expressed as changes in rotational behavior (**A**) and TH+ cell counts (**B**). Data are mean ± SD (n = 3–4 per group). *P < 0.05; **P < 0.01, ANOVA with Tukey post-hoc test.

compared with VMN grafts was also noted (Figure 6A), suggesting that Wnt5a enhances the number of TH+ cells by increasing both the number of Nurr1+ precursors and their differentiation into TH+ DA neurons. We also found that VMN-Wnt5a–derived TH+ neurons retained their midbrain identity better than control VMNs in vivo. Immunohistochemistry for paired-like homeodomain transcription factor 3 (Pitx3; a factor found only in midbrain DA neurons and important for their survival; ref. 31) and G protein–coupled inward rectifying K+ channel 2 (GIRK2; preferentially expressed in SNpc DA neurons; ref. 32) confirmed that TH+ cells within both VMN and VMN-Wnt5a grafts preserved a midbrain DA phenotype (Figure 6, E and F). Additionally, we used quantitative real-time PCR to evaluate the expression of midbrain-specific genes both in vitro (data not shown) and in tissue microdissected from the graft site in vivo (Figure 6, G–K). In VMN-Wnt5a grafts, we found trends for increased *DAT* mRNA (dopamine transporter), as well as significantly elevated expression of *TH* (5.7-fold compared with VMN grafts) and *Pitx3* mRNA, confirming the increase in DA neurons. Additionally, when VMN-Wnt5a grafts were compared with VMN grafts and intact and lesioned striatum, they showed no change in *Msx1* mRNA (expressed in proliferative DA progenitors), but a significant increase in the expression of *Lmx1a* mRNA (a transcrip-

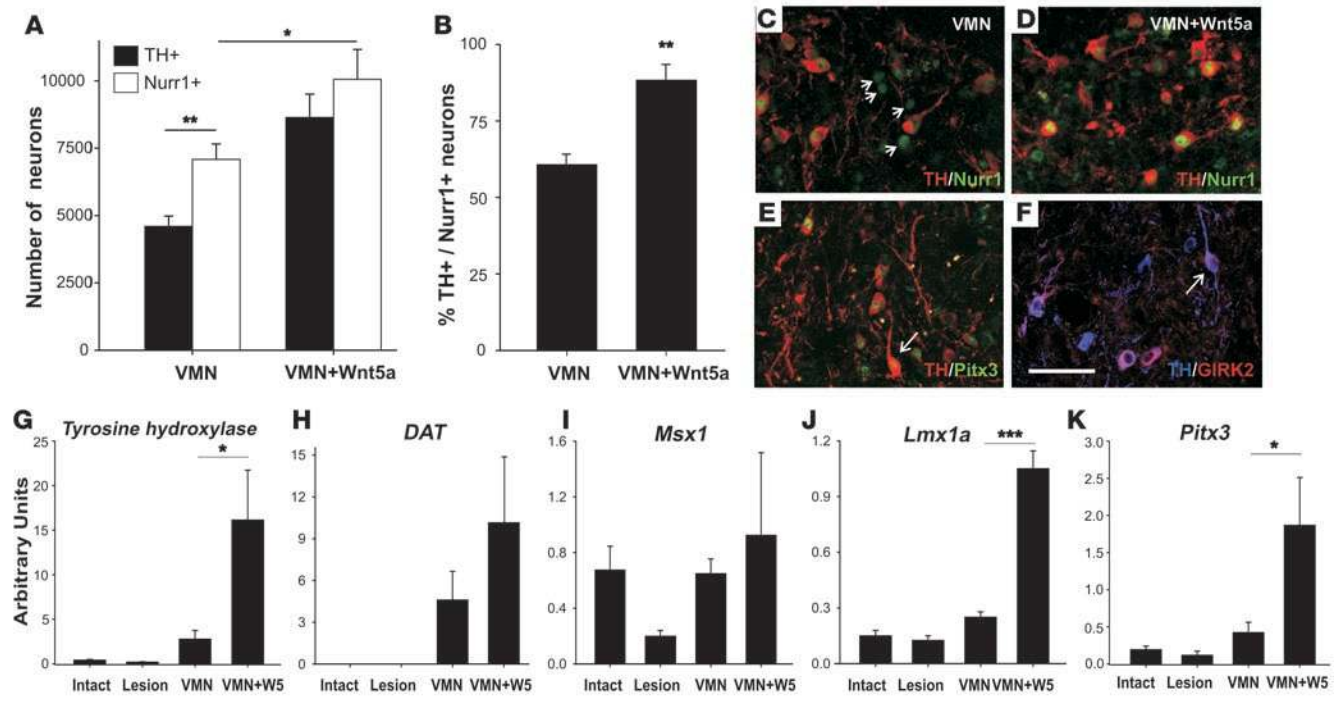

Figure 6
Improved differentiation of Nurr1+ DA precursors and expression of midbrain-specific markers by VMN-Wnt5a cells in vivo. (**A**) Number of TH+ and Nurr1+ cells within the grafts and (**B**) ratio of TH+ to Nurr1+ cells. Note there is no significant difference between TH+ and Nurr1+ cell number in VMN-Wnt5a grafts, suggesting that almost all precursor cells (i.e., 88%) adopted a DA fate (see **D**), unlike in VMN grafts alone, where numerous Nurr1+TH− cells were observed (**C**, arrows). Data are mean ± SD (n = 6 per group). *P < 0.05; **P < 0.01, Student's t test. (**E**) Pitx3/TH and (**F**) GIRK2/TH staining within the grafts confirmed midbrain phenotype. (**G**–**K**) Expression profile of midbrain DA neuron genes involved in development and function, as assessed by quantitative real-time RT-PCR. Both early and late genes in DA development were upregulated in VMN-Wnt5a grafts. Data are mean ± SD (n = 3–4 per group). *P < 0.05; ***P < 0.001, ANOVA with Tukey post-hoc test. Scale bar: 50 μm.

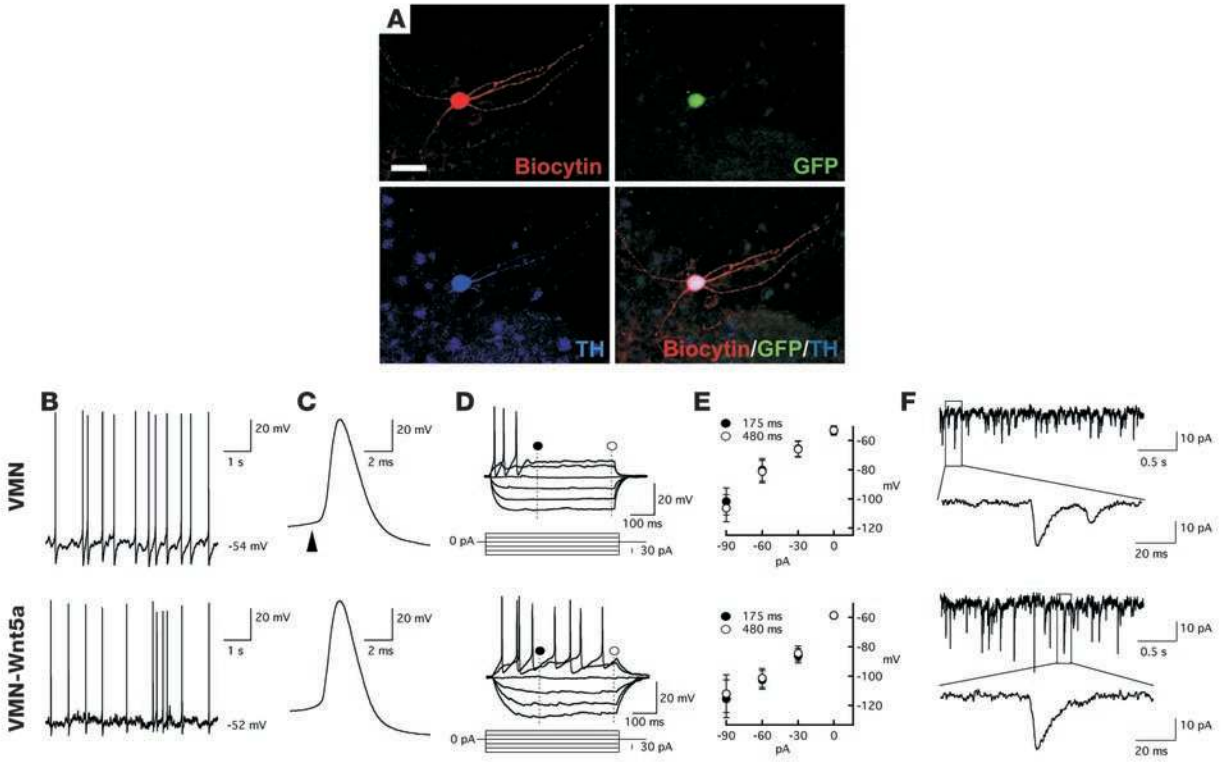

Figure 7
VMN-Wnt5a cells show the electrophysiological properties of midbrain DA neurons. (**A**) Example of triple labeling for biocytin, GFP, and TH immunoreactivity of recorded DA cell, as revealed by confocal microscopy. (**B**–**F**) No differences between control-transfected cells and cells transfected with Wnt5 were detected with respect to resting membrane potential and spontaneous firing rate (**B**); action potential threshold, amplitude, and duration (**C**); and inward rectification on hyperpolarization steps as assessed by current-voltage curves (**E**; n = 8 cells/group; mean ± SEM). Spontaneous action potential frequencies varied within both groups, ranging from 0.1 to 10 Hz. Arrowhead in **C** indicates the onset/threshold of the action potential. (**D**) In those cells that did not discharge spontaneously, action potentials were elicited by depolarizing current injections via patch pipette. (**F**) Some *TH-GFP*$^+$ cells in both groups received functional excitatory synaptic inputs, as illustrated by sEPSCs recorded at resting membrane potential in voltage-clamp mode. Insets show enlarged sEPSCs corresponding to the boxes on the upper traces.

tion factor expressed in the entire DA lineage; ref. 33). Thus, our in vivo analysis indicates that the TH$^+$ cells in VMN-Wnt5a grafts are true midbrain DA neurons and express higher levels of critical transcription factors and dopaminergic markers than do VMN grafts, suggesting a more stable and robust dopaminergic phenotype in VMN-Wnt5a grafts.

To determine whether the TH$^+$ cells derived from VMN and VMN-Wnt5a cells (cultured in the presence of FGF2/Shh/FGF8) were functional neurons, we recorded their electrophysiological properties using whole-cell patch-clamp technique. In order to identify and record from the TH$^+$ cells, VMNs were cultured from TH-GFP mice (34). TH-GFP$^+$ cells were recorded and biocytin filled (Figure 7A). The majority of the VMN-Wnt5a and control VMN cells (n = 9 and 10, respectively; Table 1) generated action potentials greater than 2 ms in duration, either spontaneously in a pacemaker-like fashion, or upon depolarizing current pulses (Figure 7, B–D). Current-voltage relations showed moderate inward rectification in response to hyperpolarization steps without any obvious delayed rectification (i.e., sag). This finding is in agreement with previously published data from the same strain of transgenic TH-GFP mice (35). Interestingly, in some of the VMN-Wnt5a and VMN cells that expressed mature DA properties, spontaneous excitatory postsynaptic currents (sEPSCs) were recorded when voltage was clamped at resting membrane potential (Figure 7F). These sEPSCs exhibited fast kinetics typical for AMPA receptor–mediated EPSCs, suggesting the occurrence of afferent excitatory glutamatergic synapses on these cells as previously described for DA neurons in vitro (36, 37). We previously found

Table 1
VMN and VMN-Wnt5a *TH-GFP*$^+$ cells express intrinsic electrophysiological properties characteristic of cultured DA cells

	VMN (n = 10)	VMN-Wnt5a (n = 9)
Input resistance (MΩ)	812 ± 135	728 ± 144
Resting membrane potential (mV)	–58.5 ± 1.7	–53.3 ± 2.9
Action potential threshold (mV)	–43.8 ± 1	–41.2 ± 1.8
Action potential amplitude (mV)	66.9 ± 5.8	71.7 ± 6.9
Action potential duration (ms)	2.1 ± 0.3	2.2 ± 0.4
Afterhyperpolarization amplitude (mV)	6.6 ± 1.0	8.1 ± 1.3
Afterhyperpolarization duration (ms)	30.3 ± 8.5	26.9 ± 4.5
Spontaneous firing frequency (Hz)	5.2 ± 2.5	2.9 ± 1.4

Values are mean ± SEM.

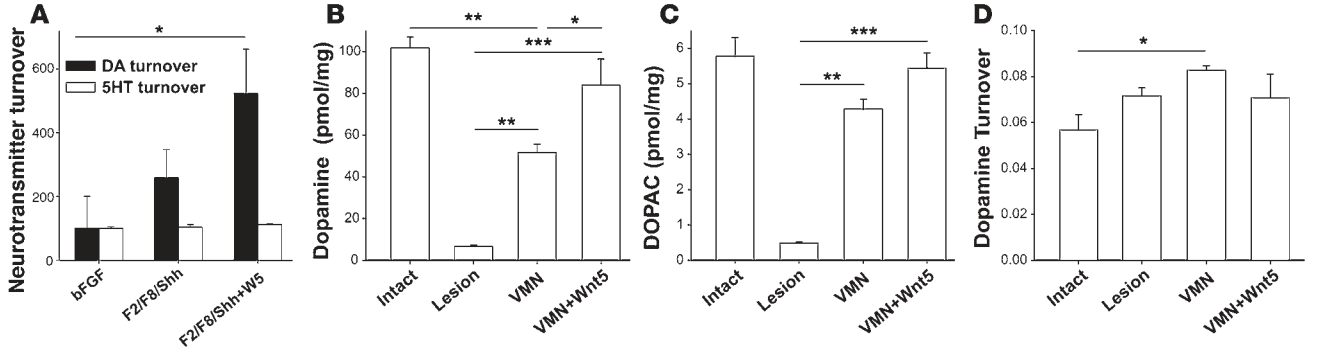

Figure 8

VMN-Wnt5a cells show midbrain dopaminergic biochemical properties in vitro and in vivo. (**A**) In vitro HPLC revealed a significant increase in DA turnover (ratio of DA to HVA) in Wnt5a-transfected cultures. This differentiation was selective for DA neurons, as it had no effect on release or turnover of other neurotransmitters, such as serotonin (not shown). Data are mean ± SD ($n = 4$ per group). *$P < 0.05$, 1-way ANOVA with Tukey post-hoc test. (**B** and **C**) HPLC revealed significantly increased DA (**B**) and DOPAC (**C**) concentration in VMN and VMN-Wnt5a striatal grafts compared with the lesion animals. VMN-Wnt5a grafts showed no significant difference in DA or DOPAC concentration compared with animals with an intact striatum. (**D**) Animals receiving VMN grafts showed a significant increase in DA turnover (ratio of DOPAC to DA) as a compensatory mechanism for the reduced DA levels, while DA turnover remained unaltered in VMN-Wnt5 grafts. Data are mean ± SEM ($n = 6$ per group). *$P < 0.05$; **$P < 0.01$; ***$P < 0.001$, ANOVA on Ranks with Dunn's post-hoc test.

that primary fetal mesencephalic TH-GFP$^+$ cells transplanted into the rat striatum exhibited intrinsic electrophysiological characteristics closely resembling those of substantia nigra DA neurons (i.e., broad action potentials, delayed inward rectifying currents and spontaneous action potentials; ref. 38). These prior results together with our present data show that the VMN-Wnt5a TH-GFP cells differentiated in vitro into functional DA neurons and expressed most of the electrophysiological properties characteristic of endogenous midbrain DA cells in vivo (39–41).

Next, the ability of the DA neurons in vitro and within grafts (400,000 cells) to synthesize, release, and use DA was assessed by reverse-phase HPLC. We found that upon KCl-induced depolarization in vitro, the levels of extracellular DA — and even more pronounced, the metabolite homovanillic acid (HVA) — were higher in spheres treated with FGF2/FGF8/Shh-Wnt5a compared with FGF2/FGF8/Shh or FGF2 alone (data not shown), demonstrating a significantly greater DA turnover (Figure 8A). It is noteworthy that noradrenaline release was not detectable, and that Wnt5a had no effect on serotonin release, serotonin metabolite (5HIAA) release (data not shown), or 5HT turnover (Figure 8A), arguing for a selective effect of Wnt5a on DA neurons. In vivo, the extensive lesioning of the nigrostriatal pathway was confirmed by the near-complete absence of DA in 6-OHDA–treated animals receiving no grafts (6.8 ± 1.3 pmol/mg, mean ± SD; Figure 8B). In VMN-Wnt5a grafts, DA levels were significantly higher compared with VMN grafts (84.1 ± 14.5 and 51.8 ± 10.0 pmol/mg, respectively), but not significantly different from those of the intact striatum (101.9 ± 11.5 pmol/mg), confirming that the cells were capable of inducing full functional recovery also at a biochemical level (Figure 8B). Similar trends were seen in DOPAC concentrations, with VMN-Wnt5a grafts showing DA metabolite (DOPAC) levels not significantly different from those of the intact striatum (Figure 8C). Only VMN grafts showed a significant increase in DA turnover (DOPAC/DA ratio; Figure 8D), suggestive of a faster DA metabolism to compensate for the denervation. This increase in turnover in vivo was not detected in VMN-Wnt5a–grafted mice, providing further evidence that their recovery at a metabolic level was complete. Thus, our results indicate that Wnt5a transfection of VMNs cultured in FGF2/FGF8/Shh enhances not only the survival and differentiation of DA precursors in vivo, but also their expression of DA transcription factors and their function in vivo at a metabolic and behavioral level.

Discussion

This study identifies what we believe to be a novel method for generating large numbers of DA neurons that possess the histological, transcriptional, biochemical, and electrophysiological profile of classical midbrain DA neurons. Exposure of VMN neural stem cells to a series of developmental cues, including Wnt5a, resulted in enhanced functional engraftment in parkinsonian mice. Further, we identified noncanonical Wnt signaling as the mechanism through which Wnt5a increases the number of Nurr1$^+$TH$^-$ precursors and their differentiation into TH$^+$ DA neurons. This effect of Wnta to induce differentiation of Nurr1 precursors via noncanonical Wnt signaling, together with the positive effect of Wnt5a on neuritogenesis and the expression of critical transcription factors (Lmx1a, Nurr1 and Pitx3), likely contributes to the functional engraftment and behavioral recovery of parkinsonian mice.

Current protocols for stem cell differentiation often include cocultivation of stem cells with other cell types, such as stromal cells (42) or astrocytes (13, 23), thus involving the exposure of stem cells to unknown signals. In the past we characterized a VM glia-derived activity that was capable of inducing dopaminergic differentiation in vitro (23) and later identified Wnt5a as part of that activity (25). More recently, astrocytes have also been found to enhance engraftment of human ES cell–derived DA neurons (13). However, VM glial cells are also the source of many different signals, including mitogens (43). Accordingly, astrocyte-treated human ES cell grafts resulted in the expansion of undifferentiated cells, with the subsequent risk of tumorigenesis (13). Similarly, we found that Shh and FGF–treated mouse ES cells showed abundant nestin$^+$ cells, cell proliferation, and sporadic formation of teratomas. Despite our protocol involving pretreatment with factors that promote proliferation, such as Shh and FGF, VMN

and VMN-Wnt5a grafts did not show cell proliferation or tumor formation, indicating that differentiation rather than expansion of proliferating progenitors was taking place in vivo.

We hereby report that VMN-Wnt5a cells (treated with FGF2/Shh/FGF8) increased the yield of VM DA neurons by 10-fold compared with bFGF-treated control neurospheres in vitro, 4-fold compared with VMN cells (treated with bFGF/Shh/FGF8) in vitro, and 2-fold compared with VMN cells in vivo. In agreement with the latter finding, we found that twice the number of VMN cells were required to achieve the same TH^+ cell numbers and level of functional recovery as obtained with VMN-Wnt5a grafts (Figure 5). Similarly, the survival of TH^+ cells in VMN-Wnt5a grafts was 50%–300% better than the survival of TH^+ cells in fetal VM tissue grafts (44, 45). Moreover, treatment of fetal VM tissue grafts with neuroprotective factors such as lazaroids (45) or neurotrophic factors such as GDNF (44) improved the number of grafted TH^+ cells but proved to be less efficient than the combined expansion and enhanced survival observed in VMN-Wnt5a grafts. Compared with the protocol described by Studer et al. (19), which also enhanced the production of TH^+ cells, our VMN-Wnt5a cultures expanded 4-fold less in vitro. However, the survival of TH^+ cells per total VMN-Wnt5a cells grafted in parkinsonian rodents was 7-fold higher. Thus, the VMN-Wnt5a protocol generated an increased yield of grafted TH^+ cells compared with previous protocols that improved engraftment over fetal tissue through progenitor expansion or neuroprotection. These findings raise the possibility that the number of donors of human fetal VM tissue required to treat a single PD patient could be reduced from 6 to 1 by the use of VMN-Wnt5a neural stem cell–derived DA neurons, possibly in combination with other approaches to increase graft survival (46). Importantly, not only did our results show that Wnt5a contributed to increased survival in vivo and the absence of tumors, but this factor also promoted the acquisition of the appropriate transcriptional profile and electrophysiological properties of midbrain DA neurons, induced greater striatal reinnervation, rescued neurotransmitter biochemistry and function, and induced complete behavioral recovery compared to VMN grafts.

Our results indicate that the VMN-Wnt5a cells fulfill both the safety and functionality criteria required for their development as a therapeutic tool for PD. The implementation of such an approach for human neural stem cells may propitiate clinical trials in which additional variables and strategies could be safely optimized. Thus, VMN-Wnt5a cells may pave the way for future clinical applications of stem cells in replacement therapies for patients with PD.

Methods

All experiments were performed according to the guidelines of the European Community and were approved by the local ethical committee (Stockholms Norra Djurförsöksetiska Nämnd, Stockholm, Sweden; N150/05 and N154/06.

VMN cultures. E10.5–E11 VM, obtained from time-mated CD-1 mice, was dissected in chilled 0.2% sucrose in PBS, mechanically dissociated, and plated at a final density of 1.25×10^5 cells/cm^2 on tissue culture plates. Serum-free N2 medium was added, consisting of a 1:1 mixture of F12 and MEM, 15 mM HEPES buffer, 1 mM glutamine, 6 mg/ml glucose (Sigma-Aldrich), 3 mg/ml Albumax, and N2 supplement (all purchased from Invitrogen). Cultures were treated with either FGF2 (20 ng/ml) or with a combination of FGF2, FGF8 (20 ng/ml each), and Shh (500 ng/ml; all purchased from R&D Systems). Cells were cultured in vitro in an incubator at 37°C with 5% CO_2 and low oxygen (3%). These hypoxic conditions (similar to those of the developing brain) have previously been shown to promote cellular proliferation and survival (47). These culturing methods resulted in the formation of neurospheres subsequently referred to as VMNs.

After 3 days, cultures were supplemented with fresh medium and at 7 days passaged using collagenase/dispase (700 μg/ml; Roche) with agitation on an orbital mixer incubator (80 rpm, 20 minutes). Cells were again plated at a density of 1.25×10^5 cells/cm^2. These cultures were referred to as passage 1. After 3 days, VMNs were transfected using Lipofectamine 2000 (according to the manufacturer's guidelines; Invitrogen) with the plasmids pCAIP2 (control plasmid; expression driven by a chicken β-actin promoter under a CMV enhancer), pCAIP2-Wnt1, or pCAIP2-Wnt5a; all transfections included a second plasmid pCAIP2-enhanced GFP. Transfection efficiency across treatments was determined by enhanced GFP expression, and no differences were observed in different experiments (data not shown). Wnt5a transfection was shown to be stable within the cultures, as revealed by immunoblot with the Wnt5a antibody at 2 and 4 days after differentiation (Supplemental Figure 1). After 4 hours, cultures were treated with sodium butyrate (1 mM) to enhance promoter activity. Twenty-four hours later, spheres were collected, resuspended in N2 media supplemented with BDNF and GDNF (30 ng/ml each; R&D Systems), plated onto poly-D-lysine– and laminin-coated plates (10 μg/ml each), and left to differentiate for 3 days. For passage 2 cultures, passage 1 spheres were split again after an additional 7 days and transfected as described above.

Rat cultures were performed as described above with the only difference being the age of the rats, which was E12.5–E12.75 at the time of dissection. Differentiated cultures were fixed in 4% paraformaldehyde for immunohistochemistry or treated with RLT/β-mercaptoethanol for RNA extraction (RNeasy Mini extraction kit; Qiagen). All differentiation experiments were performed in quadruplicate.

The effects of Wnt5a overexpression were also achieved in vitro by treatment of cultures with recombinant mouse Wnt5a protein (100 ng/ml; R&D Systems) during the period of differentiation.

For Wnt5a blocking experiments in vitro, cells were plated 4 hours after Wnt5a transfection and treated with one of the following compounds: Wnt5a antibody (2 μg/ml; R&D Systems), casein kinase 1 inhibitor D4476 (50 μg/ml; Roche), and recombinant mouse Dickkopf-1 (500 ng/ml; R&D Systems).

For clonal assaying, spheres were dissociated to a single cell suspension and plated at 1 cell/well in a 96 well plate in the presence of filtered VMN-Wnt5a–conditioned media. Single cell derived spheres were plated onto PDL/laminin and left to differentiate for 5 days prior determination of trilineage potential.

6-OHDA lesioning and transplantation. Sixty adult male CD-1 nude mice (25–35 g; Charles River Laboratories), anesthetized with 4% chloral hydrate (Sigma-Aldrich), received unilateral stereotaxic injections of 6-OHDA (3 μg; Sigma-Aldrich) into the right SNpc as previously described (48).

Primary VM was dissected from E12.25–E12.75 rats, expanded for 1 week, and transfected as described above. One day after transfection, VMNs were collected, dissociated gently with collagenase/dispase, and resuspended at a density of 100,000 cells/ml in N2 medium. Ten days after lesioning, selected animals were again anesthetized and stereotaxically injected with 2 μl of cell suspension at 2 sites (from bregma, anterior 0.7 mm, lateral 1.75 mm, ventral 2.75 and 3.75 mm, incisor bar 0 mm) according to Franklin and Paxinos (49). Cells were injected slowly through a 22-gauge, 10-μl Hamilton syringe, and the needle was left in place for 2 minutes after injection. Fourteen mice received sham grafts (4 μl N2 medium), 21 mice received FGF2/FGF8/Shh-treated VMNs overexpressing the control plasmid pCAIP2, and 21 mice received FGF2/FGF8/Shh-treated VMNs overexpressing Wnt5a. An additional 4 mice received grafts of 800,000 cells (FGF2/FGF8/Shh-treated VMNs plus control plasmid).

Eight weeks after grafting, 9–10 mice from each group were killed by an overdose of sodium pentobarbital (100 mg/kg i.p.), perfused with 25 ml 37°C 0.1 M PBS (pH 7.4), followed by 25 ml 37°C 4% paraformaldehyde (Sigma-Aldrich) in 0.1 M phosphate buffer and 0.2% picric acid (pH 7.4, 4°C) and then 25 ml 4°C 4% paraformaldehyde. Brains were removed, postfixed for 1 hour, and left overnight at 4°C in 20% sucrose and PBS solution. The following day, 18-μm-thick coronal sections were cut serially through the striatum (12 series) and 30 μm through the SNpc (3 series) and mounted directly onto superfrost slides. For counts of TH^+ and $Nurr1^+$ cells, one complete series from the striatum was costained and all immunoreactive cells within the sections were counted (the cell nuclei being used as the counting unit).

The remaining grafted animals were killed by decapitation, the brains were rapidly removed, and the striatum was dissected out on chilled plates. For 6 animals per group, the striatal tissue was transferred to a solution containing antioxidants (as described below for HPLC). For the remaining 3–4 animals per group, the striatal tissue was placed directly into RLT buffer/β-mercaptoethanol for RNA extraction (RNeasy Mini Extraction kit; QIAGEN) and subsequent quantitative RT-PCR.

Six animals received transplantation of 40,000 mouse ES cells predifferentiated in the presence of Shh, FGF2, and FGF8, according to the protocol of Barberi et al. (42). Half of these animals showed teratomas and were used as a comparison and positive control for markers of proliferating cells and tumor formation.

Behavioral testing. Lesioned animals were selected for transplantation based on amphetamine-induced (5 mg/kg) rotational behavior. Motor asymmetry was quantified 9 days after lesioning and then fortnightly after transplantation. Circling behavior was measured for 3 minutes at 15, 30, 45, and 60 minutes after injection, calculated as number of rotations per minute and expressed in Figure 3A as percent change in rotational behavior compared with pregraft behavior. Animals making greater than 7 rotations per minute (lesion greater than 90%) were selected for grafting (50). Using an additional behavioral paradigm, apomorphine rotational testing was performed to confirm functional recovery in transplanted animals (51). Apomorphine (0.25 mg/ml) was injected subcutaneously 24 hours prior to killing the animals. The number of rotations were recorded over 45 minutes; data are expressed as the net number of rotations per minute.

Immunohistochemistry and immunoblotting. Immunohistochemistry was performed on 4% paraformaldehyde fixed cultures and slides. The following primary antibodies were used: rabbit anti-TH (1:200; PelFreez), mouse anti-TH (1:100; Diasorin), Nurr-1 (1:500; Santa Cruz), mouse anti–Tuj1/βIII-tubulin (1:1,000; Promega), rabbit anti-Pitx3 (1:200; a gift from P. Burbach, Rudolf Magnus Institute of Neuroscience, Utrecht, The Netherlands), rabbit anti-GIRK2 (1:100; Chemicon), mouse anti-GFP (1:200; Chemicon), rabbit anti–phospho-histone-3 (1:200; Upstate), mouse anti–PCNA (1:100; Sigma-Aldrich), rabbit anti-Oct3/4 (1:400; Santa Cruz), rat anti-nestin (1:100; Developmental Studies Hybridoma Bank), mouse anti–Tuj1/βIII-tubulin, IgG (1:2,000; Promega), mouse anti-oligodendrocyte marker O4, IgM (1:100; Chemicon), rabbit anti-GFAP (1:200; DAKO). Appropriate fluorophore-conjugated secondary antibodies: (Cyanin-2, Cy3, and Cy5, 1:500; Jackson ImmunoResearch) were used for visualization. CyTM3-conjugated streptavidin (1:200; Jackson ImmunoResearch) was used for visualization of biocytin-filled cells following electrophysiology. Hoechst nuclear stain (5 mg/ml, 1:5,000; Sigma-Aldrich) was performed for visualization of all cells for in vitro cultures.

For immunoblotting, cells were washed and immediately frozen at –20°C. Cells were then thawed in the presence of lysis buffer (pH 8, containing 20 mM HEPES, 150 mM NaCl, 1 mM EDTA, 0.5% NP40, and 1× complete protease inhibitor; Roche) for 15 minutes at 4°C. The lysates were then centrifuged at 20,000 *g* for 20 minutes. Supernatant was collected, and protein content was measured using the Biorad Protein Assay according to the instructions of the manufacturer. Protein (20 μg per sample) was mixed with sample buffer (final concentration, Tris-HCl 62.5 mM, SDS 2%, β-mercaptoethanol 2.5%, DTT 75 mM, glycerol 10%, Bromophenol blue 0.005%). DTT 5M (1.2 μl) and dH_2O was added for a final volume of 25 μl. Samples were boiled, loaded in a 12% SDS-PAGE (BioRad ready gel Tris-HCl), and electrotransferred to a nitrocellulose membrane (Trans-Blot Transfer Medium; BioRad). For protein detection, membranes were blocked in 5% milk and incubated with goat anti-Wnt5a specific primary antibody (1:500; R&D Systems) or mouse anti–active β-catenin (1:500; Upstate) and appropriate horseradish peroxidase–conjugated secondary antibodies. β-Actin (1:5,000; BD Biosciences) was used as a control for protein loading. Signals were detected with the ECL plus system (Amersham). Recombinant mouse Wnt5a (10 ng) was run as a positive control.

Quantitative real-time RT-PCR. Real-time RT-PCR was carried out as previously described (25). Quantum RNA classical 18S internal standard was purchased from Ambion and PCR primers from DNA Technologies. Oligonucleotides sequences were as follows: TH forward, 5′-AGTACTTTGTGCGCTTCGAGGTG-3′; TH reverse, 5′-CTTGGGAACCAGGGAACCTTG-3′; Pitx3 forward, 5′-TTCCCGTTCGCCTTCAACTCG-3′; Pitx3 reverse, 5′-GAGCTGGGCGGTGAGAATACAGG-3′; Msx1 forward, 5′-GAAGATGCTCTGGTGGAAGGC-3′; Msx1 reverse, 5′-TACTGCTTCTGGCGGAACTT-3′; Lmx1a forward, 5′-CACCCCTATGGTGCTGAACC-3′; Lmx1a reverse, 5′-TGTGTCATCACTATCCAAGTCATGG-3′; DAT forward, 5′-ACTTCTACCGACTCTGTGAGGCAT-3′; DAT reverse, 5′-AGGTGGTGATGATTGCGTCTCTAT-3′.

HPLC. Dopamine levels in the intact, lesioned, VMN-transplanted and VMN-Wnt5a–transplanted striatum were determined using reverse-phase HPLC as previously described (48). For tissue preparation, the striatal tissue was dissected out on a chilled plate, weighed, and placed in 200 μl 0.4 M perchloric acid ($HClO_4$) containing 0.05% sodium metabisulphate ($Na_2S_2O_5$) and 0.01% disodium EDTA. The sample tissue was homogenized, cellular and vesicular membranes disrupted using a sonicator and finally stored at 70°C. For in vitro analysis of DA release, VMNs (F2, F2/F8/Shh, and F2/F8/Shh-Wnt5a treated) were plated for differentiation in a 12-well plate and incubated in 200 μl N2 medium supplemented with 56 mM KCl for 30 minutes. The media were then collected and stabilized with 20 μl of the same matrix used for striatal tissue. On the day of analysis, all samples were centrifuged at 10,500 *g* for 10 minutes and filtered though minispin filters for additional 3 minutes at 10,000 rpm before being injected into the HPLC.

For each sample, 25 μl was injected by a cooled autosampler (Midas) into an ESA Coulochem III coupled with an electrochemical detector. The mobile phase (sodium acetate 5 g/l, Na_2-EDTA 30 mg/l, octane-sulfonic acid 100 mg/l, methanol 10%, pH 4.2) was delivered at a flow rate of 500 μl/min to a reverse-phase C18 column (4.6 mm diameter, 150 mm length; CHROMPACK). The peaks were processed by the Azur chromatographic software. Concentrations of DA and its metabolite DOPAC, as well as 5-HT and the metabolite 5HIAA, were calculated for each sample.

Electrophysiology. Whole-cell patch-clamp recordings were performed in vitro on cultured VMN and VMN-Wnt5a $TH\text{-}GFP^+$ cells. In order to be able to identify TH^+ cells, VM was dissected from E10.5 mice expressing enhanced GFP under control of the rat TH promoter (34). Cells were cultured as described above and allowed to differentiate for 7–14 days on PDL/laminin-coated glass coverslips. Whole-cell patch-clamp recordings were made as previously described (38). In short, the coverslips with differentiated cells were transferred to a recording chamber continuously perfused at a rate of 3 ml/min, at room temperature, with gassed (95% O_2 and 5% CO_2) artificial cerebrospinal fluid containing: NaCl 119 mM; KCl 2.5 mM; $MgSO_4$ 1.3 mM; $CaCl_2$ 2.5 mM; $NaHCO_3$ 26.2 mM; NaH_2PO_4

1 mM; glucose 11 mM (292 mOsm, pH 7.4). Cells expressing GFP were identified using a wide-band excitation filter (450–480 nm), and the whole-cell patch-clamp recordings were made using infrared differential interference contrast video microscopy (BX50WI; Olympus). Recording pipette tip resistance of 3.5–5 MΩ when filled with solution containing K-gluconate 122.5 mM; KCl 17.5 mM; NaCl 8 mM; KOH-HEPES 10 mM; KOH-EGTA 0.2 mM; MgATP 2 mM; and Na_3GTP 0.3 mM (295 mOsm, pH 7.2). Whole-cell currents and voltages were amplified by a patch-clamp amplifier (EPC10; HEKA Elektronik) as described previously (38). Action potential durations were measured at half peak amplitude of the action potential. sEPSCs were detected by MiniAnalysis software (Synaptosoft). Responses were accepted as sEPSC if peak amplitudes were greater than 3 times above the average RMS baseline noise level. Biocytin was added to the pipette solution to identify the recorded cells using immunostaining.

Only 1 of 11 VMN-Wnt5a and 2 of 11 VMN TH-GFP$^+$ cells displayed electrophysiological properties generally associated with glial cells: highly negative resting membrane potentials (–78 ± 2.0 mV) and no inward or outward membrane currents during voltage steps. This finding is consistent with the proportion of TH$^+$ neurons correctly targeted with the TH-GFP reporter construct (34).

Statistics. One-way ANOVA with Tukey post-hoc tests or 2-tailed Student's *t* tests were used. A *P* value of 0.05 or less was considered significant, unless stated otherwise.

Acknowledgments

We thank Manolo Carta for assistance with HPLC, Paola Sacchetti for her assistance with the Western blots, and Lenka Bryova for animal genotyping. This work was supported by funding from Michael J. Fox Foundation, European Commission (Eurostemcells), Swedish Foundation for Strategic Research, Swedish Royal Academy of Sciences, Knut and Alice Wallenberg Foundation, Swedish MRC, and Karolinska Institutet. C.L. Parish was supported by a National Health and Medical Research (NH&MRC), Australia C.J. Martin Fellowship and a Human Frontiers Science Program Long-term fellowship (differing years). G. Castelo-Branco was supported by Praxis XXI programme of the Portuguese Fundação para a Ciência e Tecnologia, European Social Fund, Karolinska Institute, and Calouste Gulbenkian Foundation. J. Tonneson was supported by European Commission Marie Curie EST grant BIONEL.

Received for publication March 30, 2007, and accepted in revised form October 3, 2007.

Address correspondence to: Ernest Arenas, Laboratory of Molecular Neurobiology, Department of Medical Biochemistry and Biophysics, Karolinska Institute, SE-171 77 Stockholm, Sweden. Phone: 468-524-87663; Fax: 468-34-19-60; E-mail: Ernest.Arenas@ki.se.

Clare L. Parish's present address is: Howard Florey Institute, The University of Melbourne, Parkville, Victoria, Australia.

Gonçalo Castelo-Branco's present address is: Laboratory of Molecular Neurodevelopment, Department of Neuroscience, Karolinska Institute, Stockholm, Sweden.

1. Kordower, J.H., et al. 1995. Neuropathological evidence of graft survival and striatal reinnervation after the transplantation of fetal mesencephalic tissue in a patient with Parkinson's disease. *N. Engl. J. Med.* **332**:1118–1124.
2. Piccini, P., et al. 1999. Dopamine release from nigral transplants visualized in vivo in a Parkinson's patient. *Nat. Neurosci.* **2**:1137–1140.
3. Piccini, P., et al. 2000. Delayed recovery of movement-related cortical function in Parkinson's disease after striatal dopaminergic grafts. *Ann. Neurol.* **48**:689–695.
4. Olanow, C.W., et al. 2003. A double-blind controlled trial of bilateral fetal nigral transplantation in Parkinson's disease. *Ann. Neurol.* **54**:403–414.
5. Freed, C.R., et al. 2001. Transplantation of embryonic dopamine neurons for severe Parkinson's disease. *N. Engl. J. Med.* **344**:710–719.
6. Winkler, C., Kirik, D., and Bjorklund, A. 2005. Cell transplantation in Parkinson's disease: how can we make it work? *Trends Neurosci.* **28**:86–92.
7. Bjorklund, A., et al. 2003. Neural transplantation for the treatment of Parkinson's disease. *Lancet Neurol.* **2**:437–445.
8. Lindvall, O., and Bjorklund, A. 2004. Cell therapy in Parkinson's disease. *NeuroRx.* **1**:382–393.
9. Freed, C.R., et al. 2001. Transplantation of embryonic dopamine neurons for severe Parkinson's disease. *N. Engl. J. Med.* **344**:710–719.
10. Lee, S.H., Lumelsky, N., Studer, L., Auerbach, J.M., and McKay, R.D. 2000. Efficient generation of midbrain and hindbrain neurons from mouse embryonic stem cells. *Nat. Biotechnol.* **18**:675–679.
11. Kim, J.H., et al. 2002. Dopamine neurons derived from embryonic stem cells function in an animal model of Parkinson's disease. *Nature.* **418**:50–56.
12. Kawasaki, H., et al. 2000. Induction of midbrain dopaminergic neurons from ES cells by stromal cell-derived inducing activity. *Neuron.* **28**:31–40.
13. Roy, N.S., et al. 2006. Functional engraftment of human ES cell-derived dopaminergic neurons enriched by coculture with telomerase-immortalized midbrain astrocytes. *Nat. Med.* **12**:1259–1268.
14. Sonntag, K.C., et al. 2007. Enhanced yield of neuroepithelial precursors and midbrain-like dopaminergic neurons from human embryonic stem cells using the bone morphogenic protein antagonist noggin. *Stem Cells.* **25**:411–418.
15. Snyder, B.J., and Olanow, C.W. 2005. Stem cell treatment for Parkinson's disease: an update for 2005. *Curr. Opin. Neurol.* **18**:376–385.
16. Doetsch, F., Petreanu, L., Caille, I., Garcia-Verdugo, J.M., and Alvarez-Buylla, A. 2002. EGF converts transit-amplifying neurogenic precursors in the adult brain into multipotent stem cells. *Neuron.* **36**:1021–1034.
17. Tropepe, V., et al. 1999. Distinct neural stem cells proliferate in response to EGF and FGF in the developing mouse telencephalon. *Dev. Biol.* **208**:166–188.
18. Sanchez-Pernaute, R., Studer, L., Bankiewicz, K.S., Major, E.O., and McKay, R.D. 2001. In vitro generation and transplantation of precursor-derived human dopamine neurons. *J. Neurosci. Res.* **65**:284–288.
19. Studer, L., Tabar, V., and McKay, R.D. 1998. Transplantation of expanded mesencephalic precursors leads to recovery in parkinsonian rats. *Nat. Neurosci.* **1**:290–295.
20. Sawamoto, K., et al. 2001. Generation of dopaminergic neurons in the adult brain from mesencephalic precursor cells labeled with a nestin-GFP transgene. *J. Neurosci.* **21**:3895–3903.
21. Ye, W., Shimamura, K., Rubenstein, J.L., Hynes, M.A., and Rosenthal, A. 1998. FGF and Shh signals control dopaminergic and serotonergic cell fate in the anterior neural plate. *Cell.* **93**:755–766.
22. Wurst, W., and Bally-Cuif, L. 2001. Neural plate patterning: upstream and downstream of the isthmic organizer. *Nat. Rev. Neurosci.* **2**:99–108.
23. Wagner, J., et al. 1999. Induction of a midbrain dopaminergic phenotype in Nurr1-overexpressing neural stem cells by type 1 astrocytes. *Nat. Biotechnol.* **17**:653–659.
24. Castelo-Branco, G., et al. 2003. Differential regulation of midbrain dopaminergic neuron development by Wnt-1, Wnt-3a, and Wnt-5a. *Proc. Natl. Acad. Sci. U. S. A.* **100**:12747–12752.
25. Castelo-Branco, G., et al. 2006. Ventral midbrain glia express region-specific transcription factors and regulate dopaminergic neurogenesis through Wnt-5a secretion. *Mol. Cell. Neurosci.* **31**:251–262.
26. Prakash, N., et al. 2006. A Wnt1-regulated genetic network controls the identity and fate of midbrain-dopaminergic progenitors in vivo. *Development.* **133**:89–98.
27. Rawal, N., et al. 2006. Dynamic temporal and cell type-specific expression of Wnt signaling components in the developing midbrain. *Exp. Cell Res.* **312**:1626–1636.
28. Glinka, A., et al. 1998. Dickkopf-1 is a member of a new family of secreted proteins and functions in head induction. *Nature.* **391**:357–362.
29. Bryja, V., Schulte, G., and Arenas, E. 2007. Wnt-3a utilizes a novel low dose and rapid pathway that does not require casein kinase 1-mediated phosphorylation of Dvl to activate beta-catenin. *Cell Signal.* **19**:610–616.
30. Schulte, G., et al. 2005. Purified Wnt-5a increases differentiation of midbrain dopaminergic cells and dishevelled phosphorylation. *J. Neurochem.* **92**:1550–1553.
31. Smidt, M.P., Smits, S.M., and Burbach, J.P. 2004. Homeobox gene Pitx3 and its role in the development of dopamine neurons of the substantia nigra. *Cell Tissue Res.* **318**:35–43.
32. Schein, J.C., Hunter, D.D., and Roffler-Tarlov, S. 1998. Girk2 expression in the ventral midbrain, cerebellum, and olfactory bulb and its relationship to the murine mutation weaver. *Dev. Biol.* **204**:432–450.
33. Andersson, E., et al. 2006. Identification of intrinsic determinants of midbrain dopamine neurons. *Cell.* **124**:393–405.
34. Sawamoto, K., et al. 2001. Visualization, direct isolation, and transplantation of midbrain dopaminergic neurons. *Proc. Natl. Acad. Sci. U. S. A.* **98**:6423–6428.

35. Jomphe, C., et al. 2005. Use of TH-EGFP transgenic mice as a source of identified dopaminergic neurons for physiological studies in postnatal cell culture. *J. Neurosci. Methods.* **146**:1–12.
36. Joyce, M.P., and Rayport, S. 2000. Mesoaccumbens dopamine neuron synapses reconstructed in vitro are glutamatergic. *Neuroscience.* **99**:445–456.
37. Sulzer, D., et al. 1998. Dopamine neurons make glutamatergic synapses in vitro. *J. Neurosci.* **18**:4588–4602.
38. Sorensen, A.T., et al. 2005. Functional properties and synaptic integration of genetically labelled dopaminergic neurons in intrastriatal grafts. *Eur. J. Neurosci.* **21**:2793–2799.
39. Grace, A.A., and Bunney, B.S. 1983. Intracellular and extracellular electrophysiology of nigral dopaminergic neurons--2. Action potential generating mechanisms and morphological correlates. *Neuroscience.* **10**:317–331.
40. Grace, A.A., and Onn, S.P. 1989. Morphology and electrophysiological properties of immunocytochemically identified rat dopamine neurons recorded in vitro. *J. Neurosci.* **9**:3463–3481.
41. Lacey, M.G., Mercuri, N.B., and North, R.A. 1989. Two cell types in rat substantia nigra zona compacta distinguished by membrane properties and the actions of dopamine and opioids. *J. Neurosci.* **9**:1233–1241.
42. Barberi, T., et al. 2003. Neural subtype specification of fertilization and nuclear transfer embryonic stem cells and application in parkinsonian mice. *Nat. Biotechnol.* **21**:1200–1207.
43. Hall, A.C., Mira, H., Wagner, J., and Arenas, E. 2003. Region-specific effects of glia on neuronal induction and differentiation with a focus on dopaminergic neurons. *Glia.* **43**:47–51.
44. Rosenblad, C., Martinez-Serrano, A., and Bjorklund, A. 1998. Intrastriatal glial cell line-derived neurotrophic factor promotes sprouting of spared nigrostriatal dopaminergic afferents and induces recovery of function in a rat model of Parkinson's disease. *Neuroscience.* **82**:129–137.
45. Nakao, N., Frodl, E.M., Duan, W.M., Widner, H., and Brundin, P. 1994. Lazaroids improve the survival of grafted rat embryonic dopamine neurons. *Proc. Natl. Acad. Sci. U. S. A.* **91**:12408–12412.
46. Brundin, P., et al. 2000. Improving the survival of grafted dopaminergic neurons: a review over current approaches. *Cell Transplant.* **9**:179–195.
47. Studer, L., et al. 2000. Enhanced proliferation, survival, and dopaminergic differentiation of CNS precursors in lowered oxygen. *J. Neurosci.* **20**:7377–7383.
48. Parish, C.L., Finkelstein, D.I., Drago, J., Borrelli, E., and Horne, M.K. 2001. The role of dopamine receptors in regulating the size of axonal arbors. *J. Neurosci.* **21**:5147–5157.
49. Franklin, K.B.J., and Paxinos, G. 1997. *The mouse brain in stereotaxic coordinates*. 1st edition. Academic Press. San Diego, California, USA.
50. Parish, C.L., et al. 2005. Cripto as a target for improving embryonic stem cell-based therapy in Parkinson's disease. *Stem Cells.* **23**:471–476.
51. Kirik, D., et al. 2002. Reversal of motor impairments in parkinsonian rats by continuous intrastriatal delivery of L-dopa using rAAV-mediated gene transfer. *Proc. Natl. Acad. Sci. U. S. A.* **99**:4708–4713.